



DC-DC Converter Fed Maximum Power Modeling and Simulation of Distributed Generation for Photovoltaic Applications

Adel El Shahat

Engineering Science Department, Faculty of Petroleum & Mining Engineering, Suez University, Suez, Egypt.

ARTICLE INFO

Article history:

Received: 28 December 2012;

Received in revised form:

18 December 2015;

Accepted: 23 December 2015;

Keywords

Distributed generation,
Maximum Power,
DC-DC Converter,
PV Module, ANN and MATLAB.

ABSTRACT

This paper proposes Artificial Neural Network (ANN) model for the required DC-DC Converter Duty Cycle feeding Maximum Power to resistive load to be used for distributed generation (DG) applications. It proposes a PV module when coupled to a load through DC-DC Converter to supply this resistive load with the maximum power from the PV module. Some of DC-DC converters topologies are discussed in brief with concentration on Cúk and SEPIC Converters operations. The mechanism of load matching is described to give the required converter duty cycle at maximum power point (MPP). Relations in 3D figures are introduced for the most probable situations for irradiance and temperature with the corresponding PV voltage and current. Also, 3D figures for the desired duty cycle, output voltage and current of DC-DC converter to gain the maximum power to the resistive load at various irradiance and temperature values. Moreover; Artificial Neural Network (ANN) is used to implement a neural model with its algebraic function to take the probable system situations and outs the proposed converter duty cycle to give maximum power for the load. All the neural model are done with their hidden and output layers' suitable neurons numbers and suitable performance goals depending on the 3D simulation figures shown in the paper.

© 2015 Elixir All rights reserved.

1. Introduction

A PV array is usually oversized to compensate for a low power yield during winter months. This mismatching between a PV module and a load requires further over-sizing of the PV array and thus increases the overall system cost. To mitigate this problem, a maximum power point tracker (MPPT) can be used to maintain the PV module's operating point at the MPP. MPPTs can extract more than 97% of the PV power when properly optimized. A typical photovoltaic system may consist of the solar generator itself and other components that maybe any one of the following: storage elements (especially in stand-alone systems); the utility grid; power converters (DC/DC or Inverters) and associated control circuitry [1-7]. DC-DC converters are electronic devices that are used whenever we want to change DC electrical power efficiently from one voltage level to another. In all applications, we want to perform the conversion with the highest possible efficiency. DC-DC Converters are needed because unlike AC, DC can't simply be stepped up or down using a transformer. In many ways, a DC-DC converter is the DC equivalent of a transformer. They essentially just change the input energy into a different impedance level. So whatever the output voltage level, the output power all comes from the input; there's no energy manufactured inside the converter. Quite the contrary, in fact some is inevitably used up by the converter circuitry and components, in doing their job. The Boost converter is another simple power electronic converter and basically consists of a voltage source, an inductor, a power electronic switch (usually a MOS-FET or an IGBT) and a diode. It usually also has a filter capacitor to smoothen the output. Buck converters provide longer battery life for mobile systems that spend most of their time in "stand-by". Buck regulators are often used as switch-mode power supplies for baseband digital core and the power amplifier [8-13]. This paper proposes the part of DC-DC Converter coupled with resistive load and supplying it with Maximum Power as shown in figure 1.

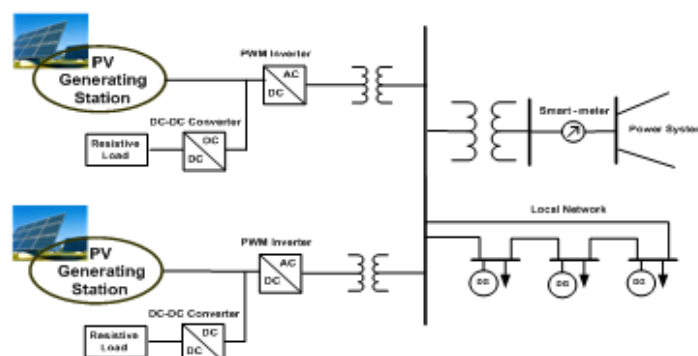


Figure (1) Simple DG System with DC-DC Converter and Resistive Load

2. Maximum Power Point for Resistive Load

When a PV module is directly coupled to a load, the PV module's operating point will be at the intersection of its I-V curve and the load line which is the I-V relationship of load. For example in figure 2, a resistive load has a straight line with a slope of $1/R_{Load}$ as shown in Figure 3. In other words, the impedance of load dictates the operating condition of the PV module. In general, this operating point is seldom at the PV module's MPP, thus it is not producing the maximum power.

A PV array is usually oversized to compensate for a low power yield during winter months. This mismatching between a PV module and a load requires further over-sizing of the PV array and thus increases the overall system cost. To mitigate this problem, a maximum power point tracker (MPPT) can be used to maintain the PV module's operating point at the MPP. MPPTs can extract more than 97% of the PV power when properly optimized. This section discusses the I-V characteristics of PV module and resistive load, matching between the two, and the use of DC-DC converters as a means of MPPT.

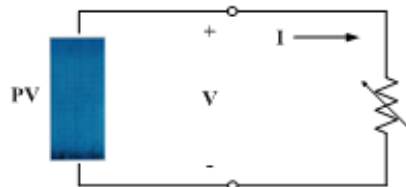


Figure (2) PV module with a resistive load.

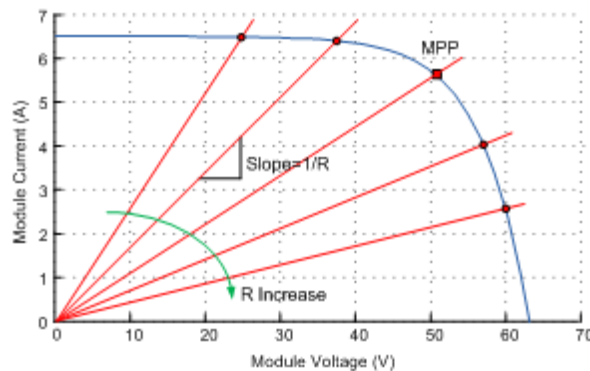


Figure (3) I-V curves of PV module and various resistive loads (1 kW/m^2 , 25°C).

3. DC-DC Converter

The heart of MPPT hardware is a switch-mode DC-DC converter. It is widely used in DC power supplies and DC motor drives for the purpose of converting unregulated DC input into a controlled DC output at a desired voltage level [14]. MPPT uses the same converter for a different purpose: regulating the input voltage at the PV MPP and providing load-matching for the maximum power transfer. There are a number of different topologies for DC-DC converters. They are categorized into isolated or non-isolated topologies.

The isolated topologies use a small-sized high-frequency electrical isolation transformer which provides the benefits of DC isolation between input and output, and step up or down of output voltage by changing the transformer turns ratio. They are very often used in switch-mode DC power supplies [15]. Popular topologies for a majority of the applications are fly-back, half-bridge, and full-bridge. In PV applications, the grid-tied systems often use these types of topologies when electrical isolation is preferred for safety reasons. Non-isolated topologies do not have isolation transformers.

These topologies are further categorized into three types: step down (buck), step up (boost), and step up & down (buck-boost). The buck topology is used for voltage step-down. In PV applications, the buck type converter is usually used for charging batteries and in LCB for water pumping systems. The boost topology is used for stepping up the voltage. The grid-tied systems use a boost type converter to step up the output voltage to the utility level before the inverter stage. Then, there are topologies able to step up and down the voltage such as: buck-boost, Cúk, and SEPIC (stands for Single Ended Primary Inductor Converter).

For PV system with batteries, the MPP of commercial PV module is set above the charging voltage of batteries for most combinations of irradiance and temperature. A buck converter can operate at the MPP under most conditions, but it cannot do so when the MPP goes below the battery charging voltage under a low-irradiance and high-temperature condition. Thus, the additional boost capability can slightly increase the overall efficiency [16].

3.1 Cúk and SEPIC Converters

The buck converter is the simplest topology and easiest to understand and design, however it exhibits the most severe destructive failure mode of all configurations [15]. Another disadvantage is that the input current is discontinuous because of the switch located at the input, thus good input filter design is essential. Other topologies capable of voltage step-down are Cúk and SEPIC. Even though their voltage step-up function is optional for LCB application, they have several advantages over the buck

converter. They provide capacitive isolation which protects against switch failure (unlike the buck topology). The input current of the Cúk and SEPIC topologies is continuous, and they can draw a ripple free current from a PV array that is important for efficient MPPT. Figure 4 shows a circuit diagram of the basic Cúk converter. It is named after its inventor. It can provide the output voltage that is higher or lower than the input voltage.

The SEPIC, a derivative of the Cúk converter, is also able to step up and down the voltage. Figure 5 shows a circuit diagram of the basic SEPIC converter. The characteristics of two topologies are very similar. They both use a capacitor as the main energy storage. As a result, the input current is continuous. The circuits have low switching losses and high efficiency [15]. The main difference is that the Cúk converter has a polarity of the output voltage reverse to the input voltage.

The input and output of SEPIC converter have the same voltage polarity; therefore the SEPIC topology is sometimes preferred to the Cúk topology. SEPIC may be also preferred for battery charging systems because the diode placed on the output stage works as a blocking diode preventing an adverse current going to PV source from the battery. The same diode, however, gives the disadvantage of high-ripple output current. On the other hand, the Cúk converter can provide a better output current characteristic due to the inductor on the output stage [14]. Therefore, this paper decides on the Cúk converter because of the good input and output current characteristics.

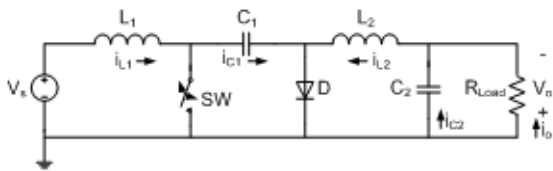


Figure (4) Circuit diagram of basic Cúk

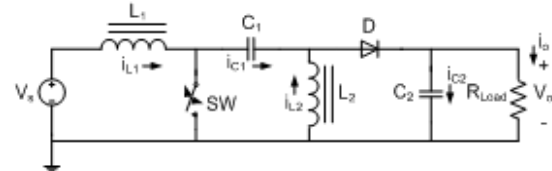


Figure (5) Circuit diagram of basic SEPIC converter.

3.2 Basic Operation of Cúk Converter

The basic operation of Cúk converter in continuous conduction mode is explained here. In steady state, the average inductor voltages are zero, thus by applying Kirchoff's voltage law (KVL) around outermost loop of the circuit shown in figure 4.

$$V_{C1} = V_s + V_o \dots (1)$$

Assume the capacitor (C_1) is large enough and its voltage is ripple free even though it stores and transfer large amount of energy from input to output [14] (this requires a good low ESR capacitor). The initial condition is when the input voltage is turned on and switch (SW) is off. The diode (D) is forward biased, and the capacitor (C_1) is being charged. The operation of circuit can be divided into two modes.

3.2.1 Mode 1: When SW turns ON, the circuit becomes one

The voltage of the capacitor (C_1) makes the diode (D) reverse-biased and turned off. The capacitor (C_1) discharge its energy to the load through the loop formed with SW , C_2 , R_{Load} , and L_2 . The inductors are large enough, so assume that their currents are ripple free. Thus, the following relationship is established.

$$-I_{C1} = I_{L2} \dots (2)$$

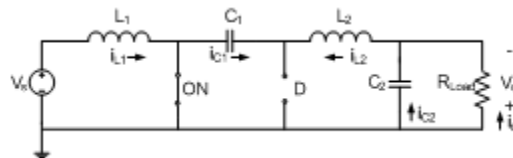


Figure (6) Basic Cúk converter when the switch is ON.

3.2.2 Mode 2: When SW turns OFF, the circuit becomes one

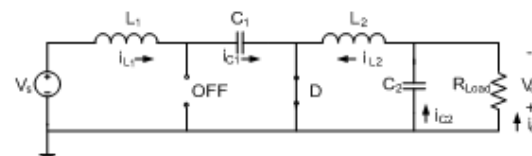


Figure (7) Basic Cúk converter when the switch is OFF

The capacitor (C_1) is getting charged by the input (V_s) through the inductor (L_1). The energy stored in the inductor (L_2) is transfer to the load through the loop formed by D , C_2 , and R_{Load} . Thus, the following relationship is established.

$$I_{C1} = I_{L1} \dots (3)$$

For periodic operation, the average capacitor current is zero. Thus, from the equation (2) and (3):

$$(I_{C1}|_{SWON}) \times DT + (I_{C1}|_{SWOFF}) \times (1-D)T = 0 \dots (4)$$

$$-I_{L2} \cdot DT + I_{L1} \cdot (1-D)T = 0 \dots (5)$$

$$I_{L1} / I_{L2} = D / (1-D) \dots (6)$$

where: D is the duty cycle ($0 < D < 1$), and T is the switching period.

Assuming that this is an ideal converter, the average power supplied by the source must be the same as the average power absorbed by the load.

$$P_{in} = P_{out} \dots (7)$$

$$V_s \cdot I_{L1} = V_o \cdot I_{L2} \dots (8)$$

$$I_{L1} / I_{L2} = V_o / V_s \dots (9)$$

Combining the equation (6) and (9), the following voltage transfer function is derived [14].

$$V_o / V_s = D / (1-D) \dots (10)$$

Its relationship to the duty cycle (D) is:

If $0 < D < 0.5$ the output is smaller than the input.

If $D = 0.5$ the output is the same as the input.

If $0.5 < D < 1$ the output is larger than the input.

3.3 Mechanism of Load Matching

As described before, when PV is directly coupled with a load, the operating point of PV is dictated by the load (or impedance to be specific). The impedance of load is described as below.

$$R_{Load} = V_o / I_o \dots (11)$$

Where: V_o is the output voltage, and I_o is the output current.

The optimal load for PV is described as:

$$R_{opt} = V_{MPP} / I_{MPP} \dots (12)$$

Where: V_{MPP} and I_{MPP} are the voltage and current at the MPP respectively. When the value of R_{Load} matches with that of R_{opt} , the maximum power transfer from PV to the load will occur. These two are, however, independent and rarely matches in practice. The goal of the MPPT is to match the impedance of load to the optimal impedance of PV. The following is an example of load matching using an ideal (loss-less) Cúk converter. From the equation (10):

$$V_s = \frac{1-D}{D} V_o \quad (13)$$

From the equation (9)

$$\frac{I_s}{I_o} = \frac{I_{L1}}{I_{L2}} = \frac{V_o}{V_s} \quad (14)$$

From the equation (13) and (14)

$$I_s = \frac{D}{1-D} I_o \quad (15)$$

From the equation (13) and (15), the input impedance of the converter is:

$$R_{in} = \frac{V_s}{I_s} = \frac{(1-D)^2}{D^2} \cdot \frac{V_o}{I_o} = \frac{(1-D)^2}{D^2} R_{Load} \quad (16)$$

As shown in figure 8, the impedance seem by PV is the input impedance of the converter (R_{in}). By changing the duty cycle (D), the value of R_{in} can be matched with that of R_{opt} . Therefore, the impedance of the load can be anything as long as the duty cycle is adjusted accordingly.

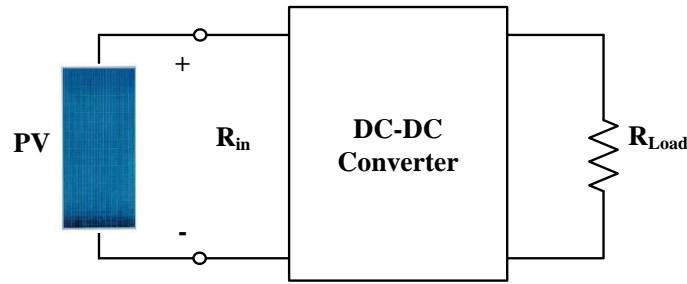


Figure (8) The impedance seen by PV is R_{in} that is adjustable by duty cycle (D).

3.4 Maximum Power Point Algorithm

The location of the MPP in the I - V plane is not known beforehand and always changes dynamically depending on irradiance and temperature. Therefore, the MPP needs to be located by tracking algorithm, which is the heart of MPPT controller. The example of resistive load matching is elaborated here to show how the output voltage and current change with varying irradiation and temperature. The maximum power transfer occurs when the input impedance of converter matches with the optimal impedance of PV module, as described in the equation below.

$$R_{in} = R_{opt} = \frac{V_{MPP}}{I_{MPP}} \quad (17)$$

The required duty cycle (D) for the Cúk converter is:

$$D = \frac{1}{1 + \sqrt{\frac{R_{in}}{R_{Load}}}} \quad (18)$$

The converter output voltage is:

$$V_o = \frac{D}{1-D} V_s \quad (19)$$

The converter output current is:

$$I_o = \frac{1-D}{D} I_s \quad (20)$$

It should be notified that, if the application requires a constant voltage, it must employ batteries to maintain the voltage constant. Also, of course, in reality DC-DC converter used in MPPT is not 100% efficient. The efficiency gain from MPPT is large, but the system needs to take efficiency loss by DC-DC converter into account. There is also tradeoff between efficiency and the cost. It is necessary for PV system engineers to perform economic analysis of different systems and also necessary to seek other methods of efficiency improvement such as the use of a sun tracker.

4. PV Cell Model

The use of equivalent electric circuits makes it possible to model characteristics of a PV cell. The method used here is implemented in MATLAB programs for simulations. The same modeling technique is also applicable for modeling a PV module. There are two key parameters frequently used to characterize a PV cell. Shorting together the terminals of the cell, the photon generated current will follow out of the cell as a short-circuit current (I_{sc}).

Thus, $I_{ph} = I_{sc}$, when there is no connection to the PV cell (open-circuit), the photon generated current is shunted internally by the intrinsic p-n junction diode. This gives the open circuit voltage (V_{oc}). The PV module or cell manufacturers usually provide the values of these parameters in their datasheets [35]. The ASE-300-DGF/50 is an industrial-grade solar power module built to the highest standards. Extremely powerful and reliable, the module delivers maximum performance in large systems that require higher voltages, including the most challenging conditions of military, utility and commercial installations.

For superior performance, quality and peace of mind, the ASE-300-DGF/50 is renowned as the first choice among those who recognize that not all solar modules are created equal [35]. The simplest model of a PV cell equivalent circuit consists of an ideal current source in parallel with an ideal diode. The current source represents the current generated by photons (often denoted as I_{ph} or I_L), and its output is constant under constant temperature and constant incident radiation of light. The PV panel is usually represented by the single exponential model or the double exponential model. The single exponential model is shown in fig. 9. The current is expressed in terms of voltage, current and temperature as shown in equation 21 [36].

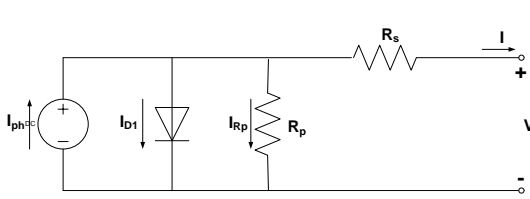


Figure (9) Single exponential model of a PV Cell.

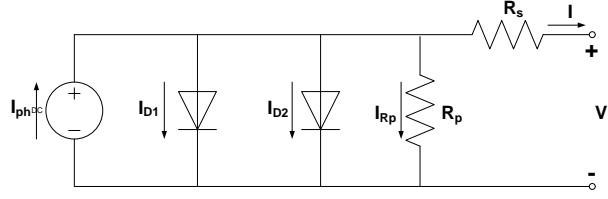


Figure (10) Double exponential model of PV Cell.

$$I = I_{ph} - I_o \left\{ \exp \left[\frac{q(V + IR_s)}{AkT} \right] - 1 \right\} - \frac{V + IR_s}{R_p} \quad (21)$$

$$I = I_{ph} - I_{s1} \left\{ \exp \left[\frac{q(V + IR_s)}{AkT} \right] - 1 \right\} - I_{s2} \left\{ \exp \left[\frac{q(V + IR_s)}{AkT} \right] - 1 \right\} - \frac{V + IR_s}{R_p} \quad (22)$$

Where I_{ph} : the photo generated current; I_o : the dark saturation current; I_{s1} : saturation current due to diffusion; I_{s2} : is the saturation current due to recombination in the space charge layer; I_{Rp} : current flowing in the shunt resistance; R_s : cell series resistance; R_p : the cell (shunt) resistance; A : the diode quality factor; q : the electronic charge, 1.6×10^{-19} C; k : the Boltzmann's constant, 1.38×10^{-23} J/K; and T : the ambient temperature, in Kelvin.

Eq.21 and Eq.22 are both nonlinear. Furthermore, the parameters (I_{ph} , I_{s1} , I_{s2} , R_s , R_{sh} and A) vary with temperature, irradiance and depend on manufacturing tolerance. Numerical methods and curve fitting can be used to estimate [36], [37].

There are three key operating points on the IV curve of a photovoltaic cell. They are the short circuit point, maximum power point and the open circuit point. At the open – circuit point on the IV curve, $V = V_{oc}$ and $I = 0$. After substituting these values in the single exponential equation (21) the equation can be obtained [36].

$$0 = I_{ph} - I_o \left\{ \exp \left[\frac{qV_{oc}}{AkT} \right] - 1 \right\} - \frac{V_{oc}}{R_p} \quad (23)$$

At the short – circuit point on the IV curve, $I = I_{sc}$ and $V = 0$. Similarly, using equation (1), we can obtain.

$$I_{sc} = I_{ph} - I_o \left\{ \exp \left[\frac{qI_{sc}R_s}{AkT} \right] - 1 \right\} - \frac{I_{sc}R_s}{R_p} \quad (24)$$

At the maximum – power point of the IV curve, we have $I = I_{mpp}$ and $V = V_{mpp}$. We can use these values to obtain the following:

$$I_{mpp} = I_{ph} - I_o \left\{ \exp \left[\frac{q(V_{mpp} + I_{mpp}R_s)}{AkT} \right] - 1 \right\} - \frac{V_{mpp} + I_{mpp}R_s}{R_p} \quad (25)$$

The power transferred to the load can be expressed as

$$P = IV \quad (26)$$

We can estimate the diode quality factor as:

$$A = \frac{V_{mpp} + I_{mpp}R_s - V_{oc}}{V_T \left\{ \ln \left(I_{sc} - \frac{V_{mpp}}{R_{sho}} - I_{mpp} \right) - \ln \left(I_{sc} - \frac{V_{oc}}{R_o} \right) + \frac{I_{mpp}}{I_{sc} - (V_{oc}/R_{so})} \right\}} \quad (27)$$

And

$$R_p = R_{sho} \quad (28)$$

$$I_o = \left(I_{sc} - \frac{V_{oc}}{R_p} \right) \cdot \exp \left(-\frac{V_{oc}}{AV_T} \right) \quad (29)$$

$$R_s = R_{so} - \frac{AV_T}{I_o} \cdot \exp \left(-\frac{V_{oc}}{AV_T} \right) \quad (30)$$

$$I_{ph} = I_{sc} \left(1 + \frac{R_s}{R_p} \right) + I_o \left(\exp \frac{I_{sc}R_s}{AV_T} - 1 \right) \quad (31)$$

As a very good approximation, the photon generated current, which is equal to I_{sc} , is directly proportional to the irradiance, the intensity of illumination, to PV cell [38]. Thus, if the value, I_{sc} , is known from the datasheet, under the standard test condition, $G_o = 1000 \text{ W/m}^2$ at the air mass (AM) = 1.5, then the photon generated current at any other irradiance, G (W/m^2), is given by:

$$I_{sc|G} = \left(\frac{G}{G_o} \right) I_{sc|G_o} \quad (32)$$

It should be notified that, in a practical PV cell, there is a series of resistance in a current path through the semiconductor material, the metal grid, contacts, and current collecting bus [39]. These resistive losses are lumped together as a series resistor (R_s). Its effect becomes very conspicuous in a PV module that consists of many series-connected cells, and the value of resistance is multiplied by the number of cells. Shunt resistance is a loss associated with a small leakage of current through a resistive path in parallel with the intrinsic device [39]. This can be represented by a parallel resistor (R_p). Its effect is much less conspicuous in a PV module compared

to the series resistance so it may be ignored [39], [40]. The ideality factor denoted as A and takes the value between one and two (as to reach the nominated characteristics) [40].

5. Photovoltaic Module Modeling

A single PV cell produces an output voltage less than 1V, thus a number of PV cells are connected in series to achieve a desired output voltage. When series-connected cells are placed in a frame, it is called as a module. When the PV cells are wired together in series, the current output is the same as the single cell, but the voltage output is the sum of each cell voltage. Also, multiple modules can be wired together in series or parallel to deliver the voltage and current level needed. The group of modules is called an array. The panel construction provides protection for individual cells from water, dust etc, as the solar cells are placed into an encapsulation of flat glass. Our case here depicts a typical connection of 216 cells that are connected in series [35]. The strategy of modelling a PV module is no different from modelling a PV cell. It uses the same PV cell model. The parameters are the all same, but only a voltage parameter (such as the open-circuit voltage) is different and must be divided by the number of cells. An electric model with moderate complexity [17] is shown in figure 3, and provides fairly accurate results. The model consists of a current source (I_{sc}), a diode (D), and a series resistance (R_s). The effect of parallel resistance (R_p) is very small in a single module, thus the model does not include it. To make a better model, it also includes temperature effects on the short-circuit current (I_{sc}) and the reverse saturation current of diode (I_o). It uses a single diode with the diode ideality factor set to achieve the best I-V curve match.

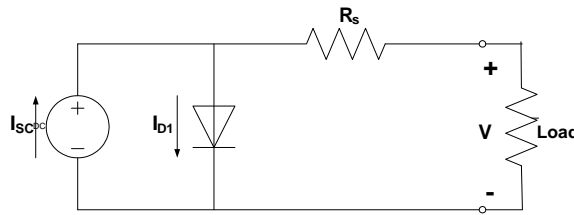


Figure (11) Equivalent circuit used in the simulations.

The equation (33) describes the current-voltage relationship of the PV cell.

$$I = I_{sc} - I_o \left(\exp\left(q \frac{V + IR_s}{AkT}\right) - 1 \right) \quad (33)$$

Where: I is the cell current (the same as the module current); V is the cell voltage = {module voltage} / {No. of cells in series}; T is the cell temperature in Kelvin (K).

First, calculate the short-circuit current (I_{sc}) at a given cell temperature (T):

$$I_{sc|T} = I_{sc|T_{ref}} [1 + a(T - T_{ref})] \quad (34)$$

Where: I_{sc} at T_{ref} is given in the datasheet (measured under irradiance of $1000W/m^2$), T_{ref} is the reference temperature of PV cell in Kelvin (K), usually $298K$ ($25^\circ C$), a is the temperature coefficient of I_{sc} in percent change per degree temperature also given in the datasheet.

The short-circuit current (I_{sc}) is proportional to the intensity of irradiance, thus I_{sc} at a given irradiance (G) is introduced by Eq. 32. The reverse saturation current of diode (I_o) at the reference temperature (T_{ref}) is given by the equation (35) with the diode ideality factor added:

$$I_o = \frac{I_{sc}}{\left(\exp\left(\frac{qV_{oc}}{AkT}\right) - 1 \right)} \quad (35)$$

The reverse saturation current (I_o) is temperature dependant and the I_o at a given temperature (T) is calculated by the following equation [41].

$$I_{o|T} = I_{o|T_{ref}} \left(\frac{T}{T_{ref}} \right)^{\frac{3}{A}} \exp\left(\frac{-qE_g}{Ak} \left(\frac{1}{T_{ref}} - \frac{1}{T} \right) \right) \quad (36)$$

The diode ideality factor (A) is unknown and must be estimated. It takes a value between one and two; however, the more accurate value is estimated by curve fitting [41] also, it can be estimated by try and error until accurate value achieved. E_g is the Band gap energy (1.12 V (Si); 1.42 (GaAs); 1.5 (CdTe); 1.75 (amorphous Si)). The series resistance (R_s) of the PV module has a large impact on the slope of the I - V curve near the open-circuit voltage (V_{oc}), hence the value of R_s is calculated by evaluating the slope dI/dV of the I - V curve at the V_{oc} [41]. The equation for R_s is derived by differentiating the I - V equation and then rearranging it in terms of R_s as introduced in equation (37).

$$R_s = - \frac{dV}{dI} \Big|_{V_{oc}} - \frac{AkT/q}{I_o \exp\left(\frac{qV_{oc}}{AkT}\right)} \quad (37)$$

Where: $\left. \frac{dV}{dI} \right|_{V_{oc}}$ is the slope of the I - V curve at the V_{oc} (using the I - V curve in the datasheet then divide it by the number of cells in series); V_{oc} is the open-circuit voltage of cell (Dividing V_{oc} in the datasheet by the number of cells in series). Finally, the equation of I - V characteristics is solved using the Newton's method for rapid convergence of the answer, because the solution of current is recursive by inclusion of a series resistance in the model [41]. The Newton's method is described as:

$$x_{n+1} = x_n - \frac{f(x_n)}{f'(x_n)} \quad (38)$$

Where: $f'(x)$ is the derivative of the function, $f(x) = 0$, x_n is a present value, and x_{n+1} is a next value.

$$f(I) = I_{sc} - I - I_o \left(\exp\left(q\left(\frac{V + IR_s}{AkT}\right)\right) - 1 \right) = 0 \quad (39)$$

By using the above equations the following output current (I) is computed iteratively.

$$I_{n+1} = I_n - \frac{I_{sc} - I_n - I_o \left(\exp\left(q\left(\frac{V + I_n R_s}{AkT}\right)\right) - 1 \right)}{-1 - I_o \left(\frac{qR_s}{AkT} \right) \exp\left(q\left(\frac{V + I_n R_s}{AkT}\right)\right)} \quad (40)$$

The figures of I - V characteristics at various module temperatures are simulated with the MATLAB model for our PV module are shown. Also, the P - V relations at various module temperatures are presented. All of these are done at various irradiance values are introduced.

6. Simulation Results

The calculation results are presented by two ways: one in 2D figures, and other with the use of 3D figures. These results are based on PV module data and the MATLAB simulation model which implemented in previous section. Relations between all possible predicted resistances values for all the entire I - V curves with the desired optimum resistance values are presented at the first from figure 11 to figure 14. We want the converter to make the load matching at the points of intersections between the curves for the most probable global values of the load resistances and the straight lines of optimum load values in order to transfer the required maximum power for the resistive load.

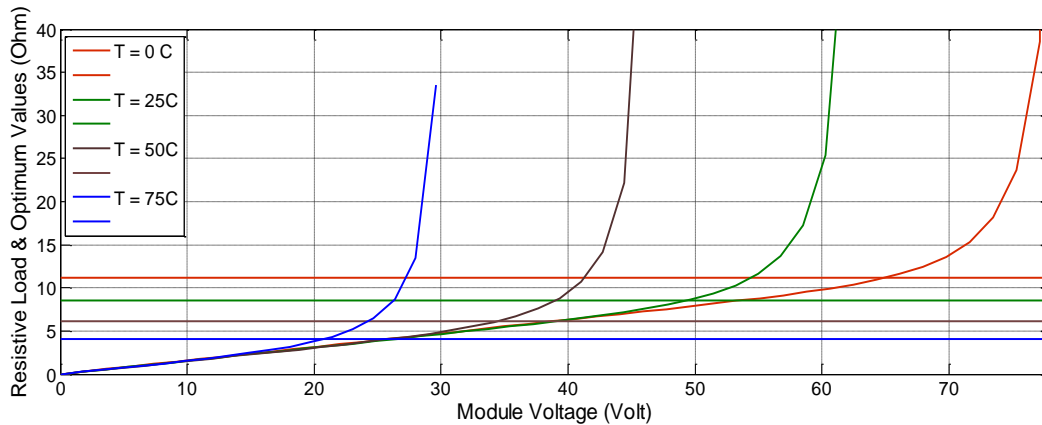


Figure (11) Resistive load and Optimum resistance values with Voltage at 1 kW/m² Irradiance.

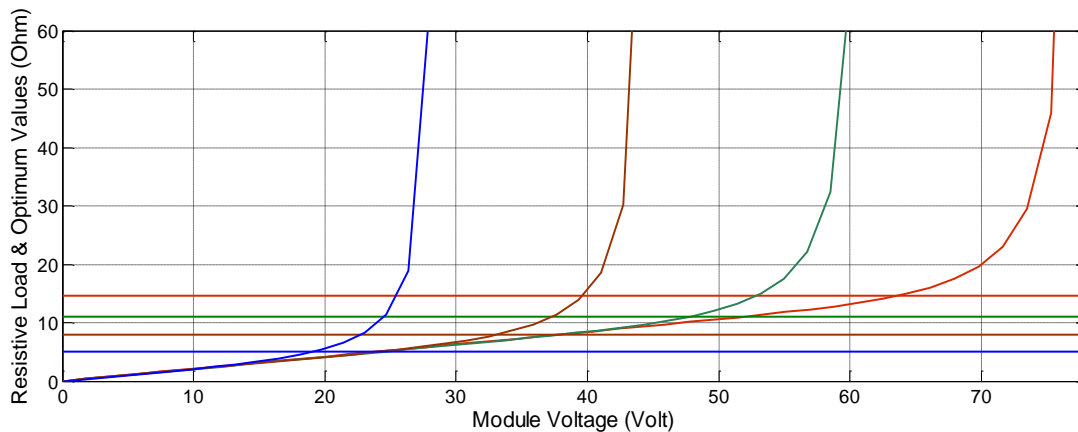


Figure (12) Resistive load and Optimum resistance with Voltage at 0.75 kW/m² Irradiance.

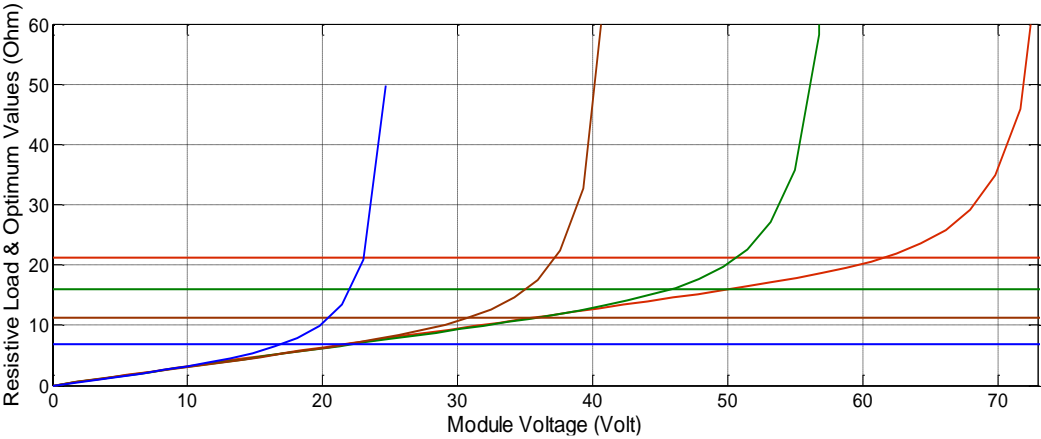


Figure (13) Resistive load and Optimum resistance with Voltage at 0.50 kW/m² Irradiance.

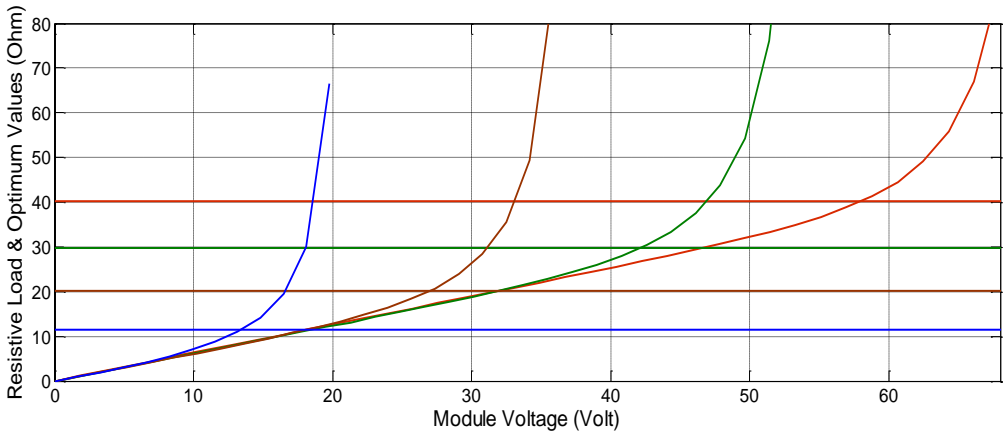


Figure (14) Resistive load and Optimum resistance with Voltage at 0.25 kW/m² Irradiance.

After that, a set of 3 D figures (from fig. 15 to fig. 22) are proposed to cover the most probable situations at various irradiance, various temperature with the current, and the voltage of the PV module. These surface faces relations will be considered later as the input learning or training data for the proposed neural network model. All these figures are based on the MATLAB PV module modeling introduced before.

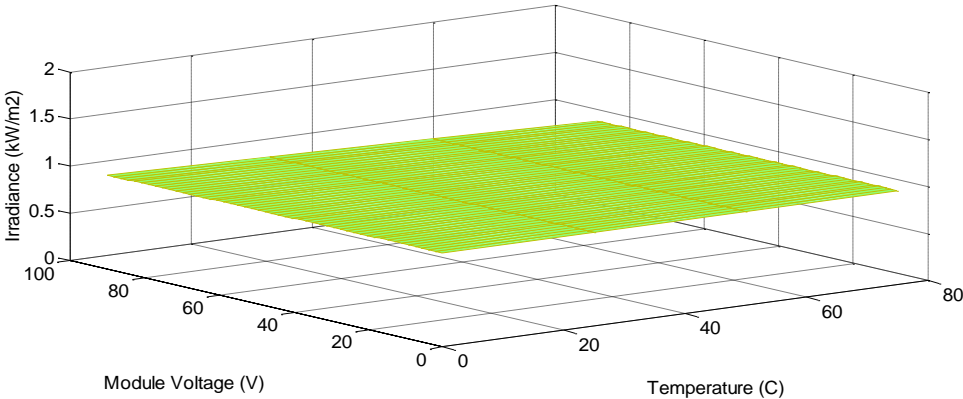


Figure (15) Voltage & Temp.& (1kW/m²) Irradiance.

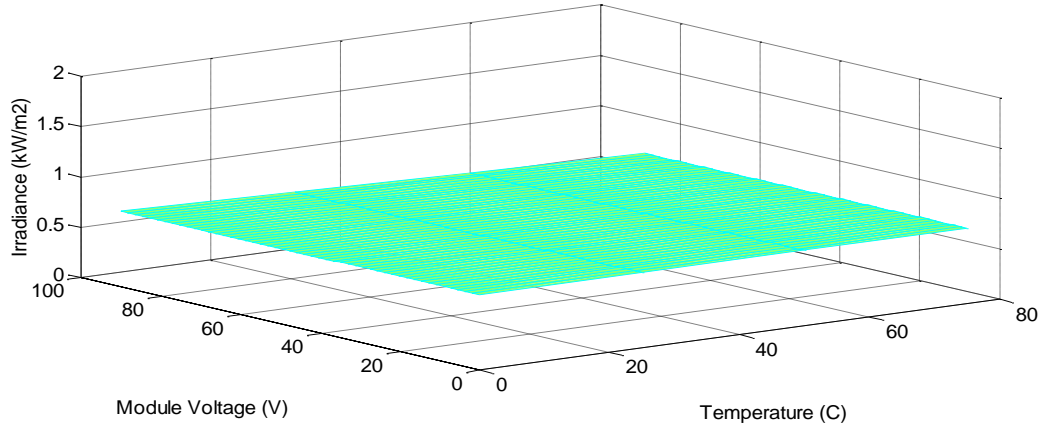
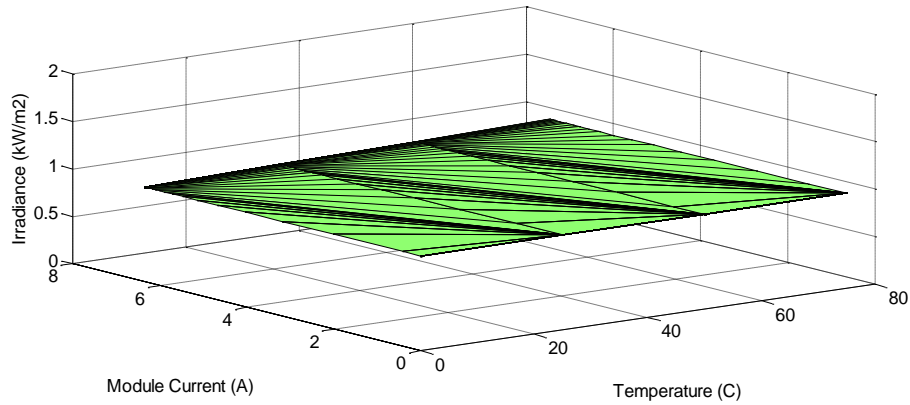


Figure (17) Voltage & Temperature& (0.75kW/m²) .

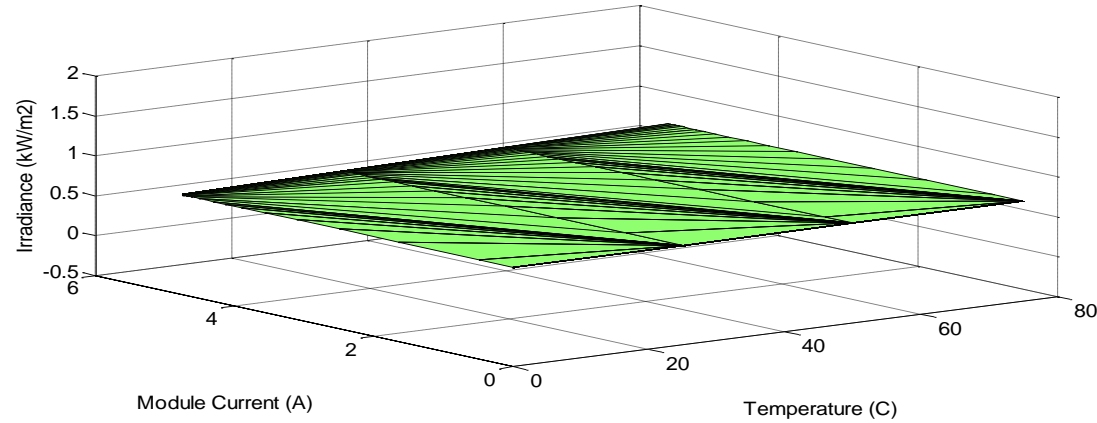


Figure (18) Current & Temperature&(0.75kW/m²) .

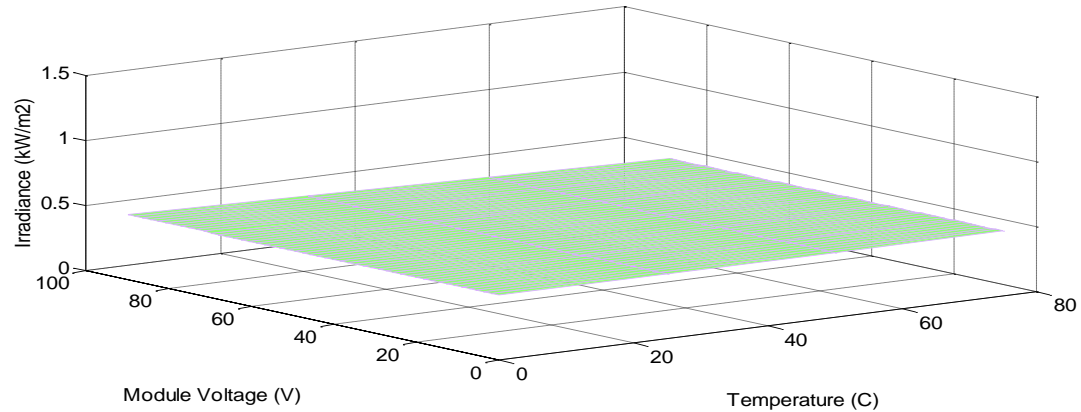


Figure (19) Voltage & Temperature&(0.50kW/m²) .

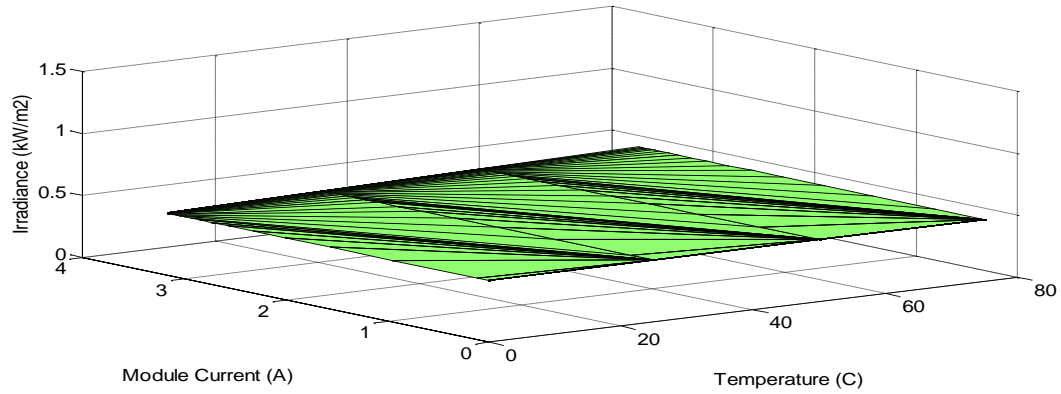


Figure (20) Current & Temperature&(0.50kW/m²) .

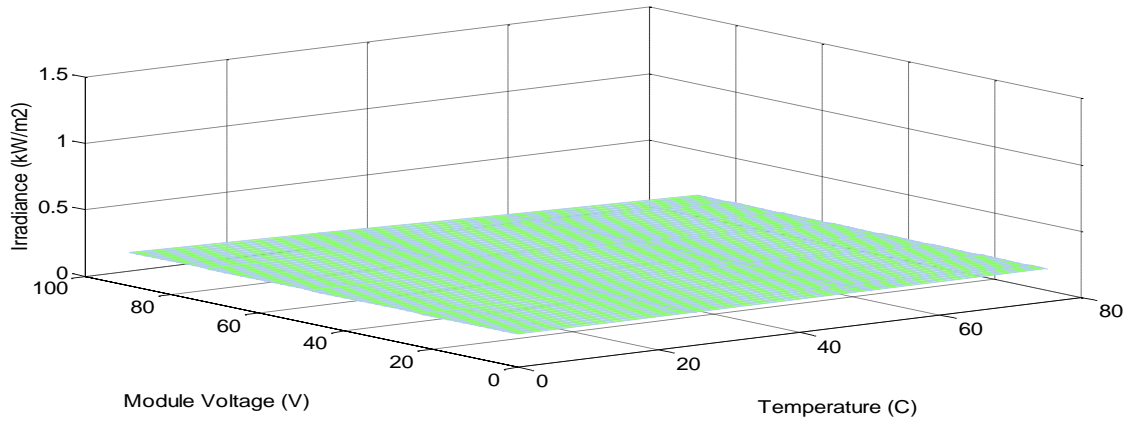


Figure (21) Voltage & Temperature&(0.25kW/m²) .

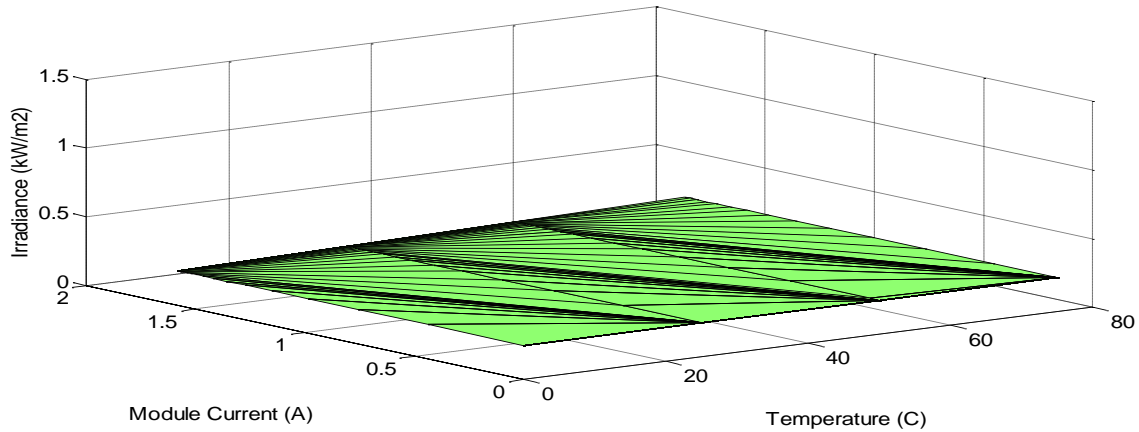


Figure (22) Current & Temperature&(0.25kW/m²).

Finally, the relations of converter duty cycle, converter output voltage, and converter output current values to transfer the maximum power from the PV module to various values of resistive loads. The converter duty cycle values from these relations are taken as target or output values. These relations are presented with variable values of temperature and irradiance in figures from 23 to 26.

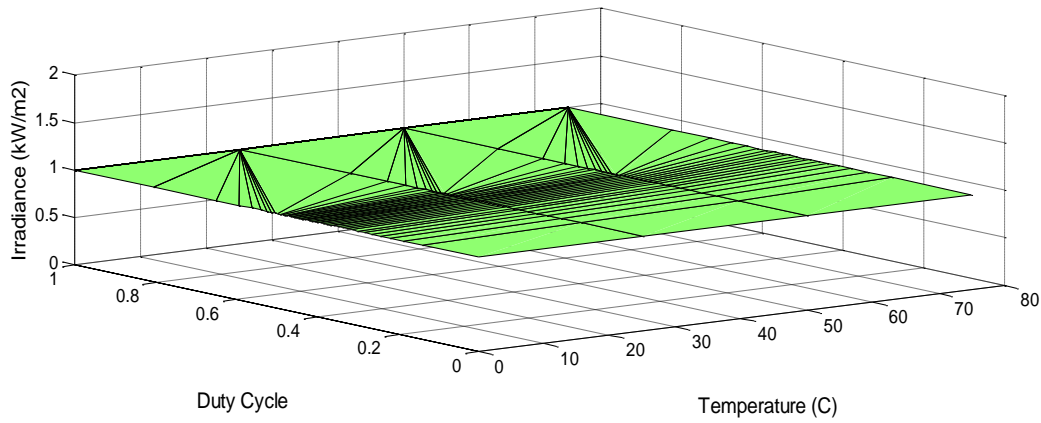


Figure (23) Converter Duty Cycle for max power with Temperature and 1 kW/m² Irradiance.

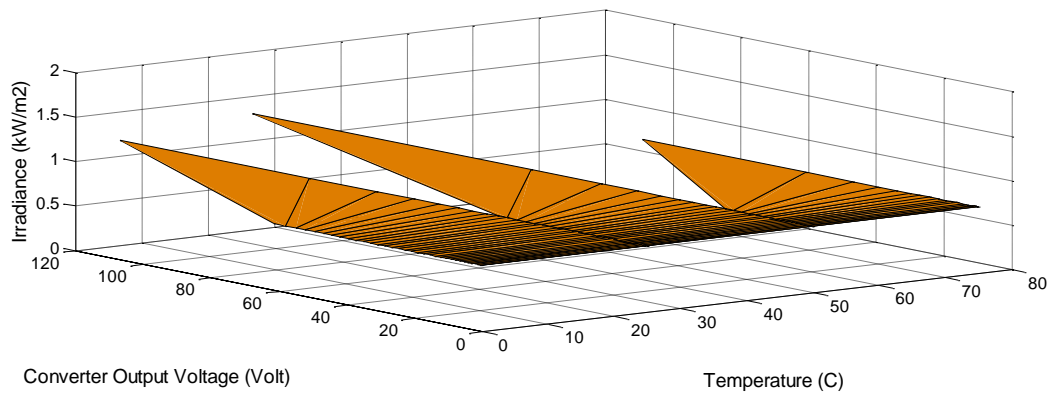


Figure (24) Converter Output Voltage for max. power with Temp. and 0.75 kW/m² Irradiance.

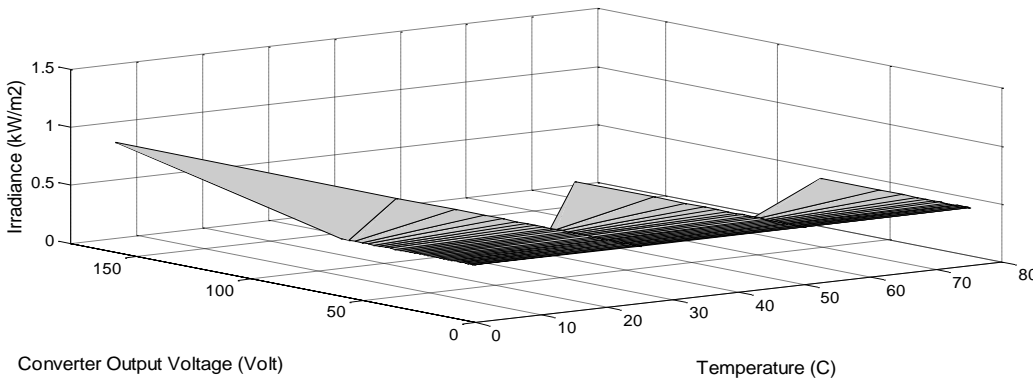


Figure (25) Converter Output Voltage for max. power with Temp. and 0.50 kW/m² Irradiance.

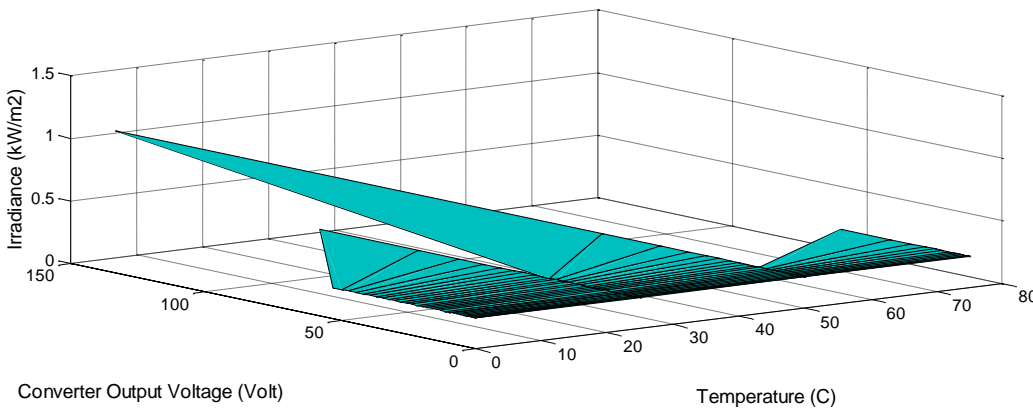


Figure (26) Converter Output Voltage for max. power with Temp. and 0.25 kW/m² Irradiance.

7. Artificial Neural Networks (ANNs) Technique

An ANN consists of very simple and highly interconnected processors called neurons. The neurons are connected to each other by weighted links over which signals can pass. Each neuron receives multiple inputs from other neurons in proportion to their connection weights and generates a single output which may propagate to several other neurons [17]. Among the various kinds of ANNs that exist, the Back-propagation learning algorithm has become the most popular used method in engineering application. It can be applied to any feed-forward network with differentiable activation functions [18], and it is the type of network used in this paper.

7.1 Fundamentals of Neural Network

The ANN modeling is carried out in two steps; the first step is to train the network, whereas the second step is to test the network with data, which were not used for training. It is important that all the information the network needs to learn is supplied to the network as a data set. When each pattern is read, the network uses the input data to produce an output, which is then compared to the training pattern. If there is a difference, the connection weights are altered in such a direction that the error is decreased. After the network has run through all the input patterns, if the error is still greater than the maximum desired tolerance, the ANN runs through all the input patterns repeatedly until all the errors are within the required tolerance [19], [20].

7.2 Data Collection, Analysis and Processing

Quality, availability, reliability, repeatability, and relevance of the data used to develop and run the system is critical to its success. Data processing starts from the data collections and analysis followed by pre-processing and then feeds to the neural network.

7.3 Network Structure Design

Though theoretically there exists a network that can simulate a problem to any accuracy, there is no easy way to find it. To define an exact network architecture such as how many hidden layers should be used, how many units should there be within a hidden layer for a certain problem is a painful job.

7.3.1 Number of Hidden Layers

Because networks with two hidden layers can represent functions with any kind of shapes, there is no theoretical reason to use networks with more than two hidden layers. In general, it is strongly recommended that one hidden layer be the first choice for any feed-forward network design [17-20].

7.3.2 Number of Hidden Units (node)

Another important issue in designing a network is how many units to place in each layer. Using too few units can fail to detect the signals fully in a complicated data set, leading to under fitting. Using too many units will increase the training time, perhaps so much that it becomes impossible to train it adequately in a reasonable period of time. The best number of hidden units depends on many factors – the numbers of input and output units, the number of training cases, the amount of noise in the targets, the complexity of the error function, the network architecture, and the training algorithm. The best approach to find the optimal number of hidden units is trial and error.

7.3.3 Initializing Back-Propagation feed-forward network

Back-propagation is the most commonly used method for training multi-layer feed-forward networks. For most networks, the learning process is based on a suitable error function, which is then minimized with respect to the weights and bias. The algorithm for evaluating the derivative of the error function is known as back-propagation, because it propagates the errors backward through the network.

8. ANN Required Duty Cycle Model with its regression function

All the neural models in this section use the previous technique which used and verified before like in [22-34] for the author in the field of green energy. First, ANN PV module model is presented with its regression function which is verified before by the author [42]. This model uses the previous 3D graphs illustrated before as training or learning data for input and desired target. The inputs in this model are the Irradiance and Temperature; the outputs are: Module Voltage, Current, and Power. This model with its hidden and output layers' suitable neurons numbers is depicted in figure 27. Also, the general neural network, and training state are presented in figures 35, and 36 respectively. This model would be used in some cases to help in predicting the required duty cycle as it will be seen.

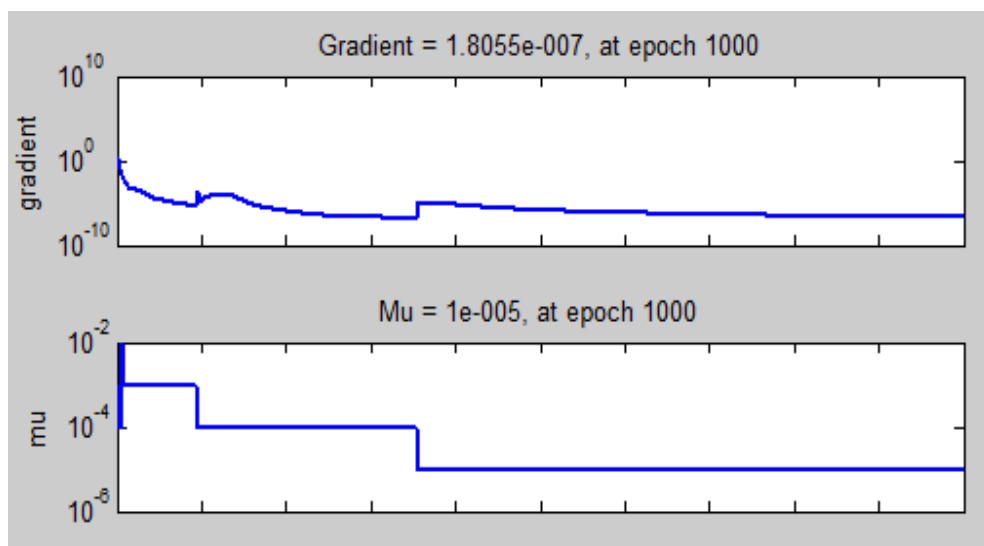


Figure (27) Training State.

$$G_n = (G - 0.6250) / (0.2797) \quad (41)$$

$$T_n = (T - 37.5000) / (27.9683) \quad (42)$$

$$E1 = -0.3884 G_n - 0.8968 T_n + 2.8411 \quad (43)$$

$$F1=1/(1+\exp(-E1)) \quad (15)$$

$$E_2 = 10.8336 G_n - 0.1120 T_n - 4.7062 \quad (44)$$

$$F2 = 1 / (1 + \exp(-E2)) \quad (11)$$

$$E_3 = -0.3773 G_n - 9.6071 T_n + 7.2495 \quad (45)$$

$$F3 = 1 / (1 + \exp(-E3)) \quad (12)$$

$$E_4 = -0.0696 G_n - 9.4705 T_n - 5.0369 \quad (46)$$

$$F4 = 1 / (1 + \exp(-E4)) \quad (14)$$

$$E5 = 6.3252 G_n + 0.3523 T_n + 4.6963 \quad (47)$$

$$F5 = 1 / (1 + \exp(-E5)) \quad (17)$$

$$E_6 = -0.1062 G_n + 3.4660 T_n + 8.7149 \quad (48)$$

$$F6=1/(1+\exp(-E6)) \quad (15)$$

$$E7 = 0.1802 G_n + 4.0327 T_n + 3.7157 \quad (49)$$

$$F7 = 1 / (1 + \exp(-E7)) \quad (17)$$

$$E_8 = 11.6503 G_n - 1.1094 T_n + 11.1433 \quad (50)$$

$$F8=1/(1+\exp(-E8)) \quad (5-5)$$

$$E_9 = 0.2372 G_n - 0.8735 T_n + 0.7613 \quad (51)$$

$$F9 = 1 / (1 + \exp(-E9)) \quad (51)$$

$$V_n = 0.0466 F1 + 0.0080 F2 + 0.0661 F3 - 0.2311 F4 - 0.0071 F5 + 2.5608 F6 + 0.0771 F7 + 0.0091 F8 - 0.0217 F9 - 2.7656 \quad (52)$$

$$I_n = 6.2907 F1 + 1.5501 F2 + 0.2881 F3 + 1.8330 F4 - 1.1986 F5 - 0.6123 F6 - 1.2526 F7 + 1.6547 F8 - 2.6831 F9 - 6.1682 \quad (53)$$

$$P_n = 7.2249 F_1 + 1.7820 F_2 + 1.0262 F_3 + 5.1377 F_4 - 1.3507 F_5 - 0.9574 F_6 + 3.4515 F_7 + 1.8830 F_8 - 6.9036 F_9 - 7.3615 \quad (54)$$

$$V = 25.2226 V_n + 42.6563 \quad (55)$$

$$I = 2.1788 I_n + 2.3181 \quad (56)$$

$$P = 57.5303 P_n + 81.4030 \quad (57)$$

Then, the first ANN model for predicting the required duty cycle for maximum power supply is presented as follow. The inputs in this model are the Irradiance and Temperature; the output is the required duty cycle to drive the DC/DC converter at maximum power transfer for the resistive load matching. This model with its hidden and output layers' suitable neurons numbers is well depicted in figure 28. Also, the general neural network, and training state are presented in figures 35, and 38 respectively.

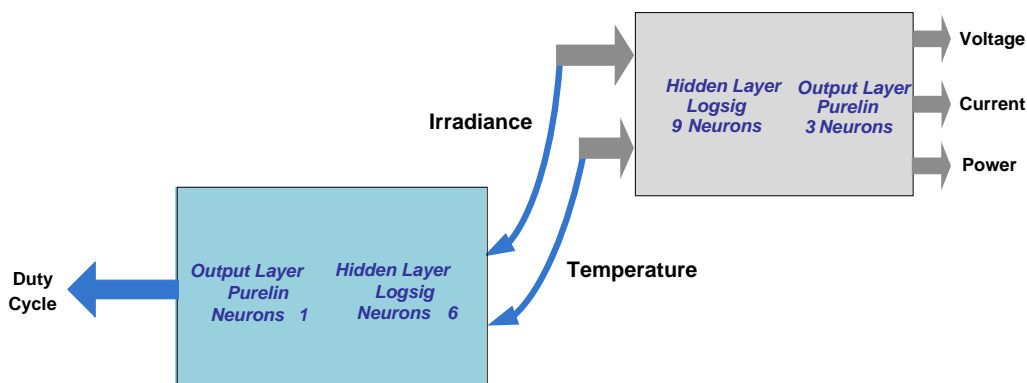


Figure (28) Duty cycle ANN Model.

The algebraic equation of this neural model is deduced as the following:

$$E1 = -0.3590 G_n - 0.3814 T_n + 0.3804 \quad (58)$$

$$F1 = 1 / (1 + \exp(-E1)) \quad (59)$$

$$E2 = -0.0141 G_n - 6.4507 T_n + 3.8184 \quad (59)$$

$$F2 = 1 / (1 + \exp(-E2)) \quad (60)$$

$$E3 = -0.0351 G_n - 0.9089 T_n - 0.9329 \quad (60)$$

$$F3 = 1 / (1 + \exp(-E3)) \quad (61)$$

$$E4 = 8.5133 G_n + 4.3558 T_n + 2.4202 \quad (61)$$

$$F4 = 1 / (1 + \exp(-E4)) \quad (62)$$

$$E5 = 5.6139 G_n + 0.2623 T_n + 3.4972 \quad (62)$$

$$F5 = 1 / (1 + \exp(-E5)) \quad (63)$$

$$E6 = -9.6390 G_n - 4.2841 T_n - 4.0081 \quad (63)$$

$$F6 = 1 / (1 + \exp(-E6)) \quad (64)$$

$$D_n = 0.6425 F1 - 0.3052 F2 - 1.8018 F3 - 0.0027 F4 - 0.1021 F5 - 0.0181 F6 + 0.4733 \quad (64)$$

$$D = 0.3087 D_n + 0.6542 \quad (65)$$

After that, the second ANN model for predicting the required duty cycle for maximum power supply is presented as follow. The inputs in this model are the module voltage and module current; the output is the required duty cycle to drive the DC/DC converter at maximum power transfer for the resistive load matching. This model with its hidden and output layers' suitable neurons numbers is well depicted in figure 29.

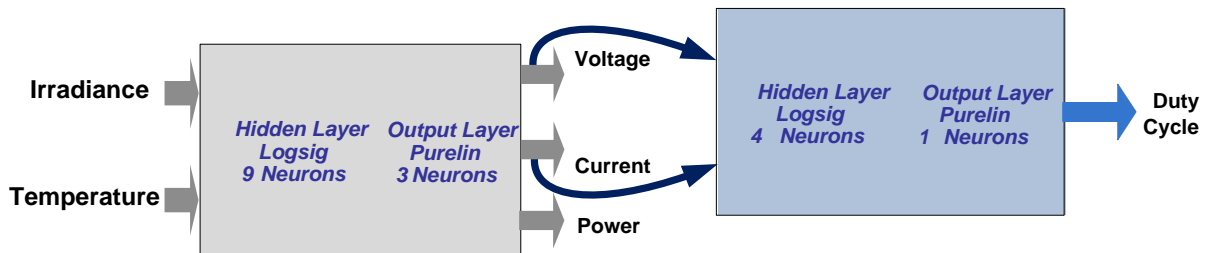


Figure (29) Duty cycle ANN Model.

The algebraic equation of this neural model is deduced as the following:

The normalized inputs V_n : (Normalized Voltage); I_n : (Normalized Current) are as follow:

$$V_n = (V - 42.6563) / (25.2226) \quad (66)$$

$$I_n = (I - 2.1788) / (2.3181) \quad (67)$$

Equations (66) and (67) present the normalized inputs for irradiance and temperature, also the following equations lead to the required derived outputs equations.

$$E1 = 0.1708 V_n - 0.0757 I_n - 3.5535 \quad (68)$$

$$F1 = 1 / (1 + \exp(-E1)) \quad (69)$$

$$E2 = -0.3229 V_n - 6.6072 I_n - 5.9777 \quad (69)$$

$$F2 = 1 / (1 + \exp(-E2)) \quad (70)$$

$$E3 = 20.3367 V_n + 0.0538 I_n + 38.8185 \quad (70)$$

$$F3 = 1 / (1 + \exp(-E3)) \quad (71)$$

$$E4 = -4.3491 V_n - 0.2479 I_n - 6.2840 \quad (71)$$

$$F4 = 1 / (1 + \exp(-E4)) \quad (72)$$

The normalized outputs are:

$$D_n = 39.5715 F1 + 2.7944 F2 + 56.3549 F3 - 0.9435 F4 - 57.9687 \quad (72)$$

The un- normalized out puts

$$D = 0.3087 D_n + 0.6542 \quad (73)$$

Finally, the third ANN model for predicting the required duty cycle for maximum power supply is presented as follow. The inputs in this model are the irradiance, temperature, module voltage and module current; the output is the required duty cycle to drive the DC/DC converter at maximum power transfer for the resistive load matching. The algebraic equation of this neural model is deduced as the following:

The normalized inputs G_n : (Normalized Irradiance); T_n : (Normalized Temperature); V_n : (Normalized Voltage); I_n : (Normalized Current) are as follow:

$$G_n = (G - 0.6250) / (0.2797) \quad (74)$$

$$T_n = (T - 37.5000) / (27.9683) \quad (75)$$

$$V_n = (V - 42.6563) / (25.2226) \quad (76)$$

$$I_n = (I - 2.1788) / (2.3181) \quad (77)$$

Equations (74), (75), (76) and (77) present the normalized inputs for irradiance, temperature, voltage, and current. The following equations lead to the required derived outputs equations.

$$E1 = 0.5936 G_n - 0.0564 T_n + 1.2431 V_n - 0.6579 I_n + 4.8487 \quad (78)$$

$$F1 = 1 / (1 + \exp (- E1))$$

$$E2 = 0.5943 G_n - 0.0479 T_n + 1.2037 V_n - 0.6658 I_n + 5.5987 \quad (79)$$

$$F2 = 1 / (1 + \exp (- E2))$$

$$E3 = -1.5461 G_n + 9.1499 T_n + 12.5644 V_n + 4.8012 I_n - 7.1509 \quad (80)$$

$$F3 = 1 / (1 + \exp (- E3))$$

The normalized outputs are:

$$D_n = 1.0e+003 * (- 0.5322 F1 + 1.1651 F2 + 0.0014 F3) - 633.1165 \quad (81)$$

The un- normalized out puts

$$D = 0.3087 D_n + 0.6542 \quad (82)$$

9. Conclusion

This paper introduces Cúk DC-DC converter coupled to resistive load by maximum power from PV module. Relations which govern the process of load matching are discussed to give the required converter duty cycle at maximum power point (MPP). The simulation results are introduced by two ways first by 2D figures for the optimum resistive load values and for the predicted whole probable range of resistive loads to give a point of view about the intersection between them i.e. point of MPP. Second, the rest of the results are well depicted in the form of 3D figures for the PV module relations I-V with the various values of irradiance and temperature based on PV module data and the implemented MATLAB simulation model. Then, the relations of converter duty cycle, converter output voltage, and converter output current values to transfer the maximum power from the PV module to various values of resistive loads with variable values of temperature and irradiance. The neural network has the ability to deal with previous relations as surface or mapping face, due to this technique ability for interpolation between points with each other and also curves.

This neural network unit is implemented, using the back propagation (BP) learning algorithm due to its benefits to have the ability to predict values in – between learning values, also make interpolation between learning curves data. This is done with suitable number of network layers and neurons at minimum error and precise manner. The ANN regression function for each unit is introduced to be used directly without operating the neural model each times. First, ANN PV module model is presented with its regression function, its inputs are the Irradiance and Temperature; the outputs are: Module Voltage, Current, and Power. Then, the first ANN model for predicting the required duty cycle for maximum power supply is introduced with its regression function, its inputs the Irradiance and Temperature; the output is the required duty cycle to drive the DC/DC converter at maximum power transfer for the resistive load matching. After that, the second ANN model for predicting the required duty cycle for maximum power supply is illustrated with its regression function, its inputs are the module voltage and module current; the output is the required duty cycle to drive the DC/DC converter at maximum power transfer for the resistive load matching. Finally, the third ANN model for predicting the required duty cycle for maximum power supply is proposed with its regression function, its inputs are the irradiance, temperature, module voltage and module current; the output is the required duty cycle to drive the DC/DC converter at maximum power transfer for the resistive load matching.

References

- [1] T. Markvart and L. Castaner, Practical Handbook of Photovoltaics, Fundamentals and Applications. Elsevier, 2003.
- [2] K. Hussein, I. Muta, T. Hoshino, and M. Osakada, "Maximum photovoltaic power tracking: an algorithm for rapidly changing atmospheric conditions," Generation, Transmission and Distribution, IEE Proceedings-, vol. 142, pp. 59–64, Jan 1995.

- [3] Hohm, D. P. & M. E. Ropp "Comparative Study of Maximum Power Point Tracking Algorithms" Progress in Photovoltaics: Research and Applications November 2002, page 47-62
- [4] G.Walker, "Evaluating mppt converter topologies using a matlab pv model," Journal of Electrical and Electronics Engineering, vol. 21, no. 1, p. 4956, 2001.
- [5] Adel El Shahat, "Maximum Power Point Genetic Identification Function for Photovoltaic System", International Journal of Research and Reviews in Applied Sciences, June 2010, (In Press).
- [6] Min Dai, M.N. Marwali, Jin-Woo Jung, A. Keyhani, "A Three-Phase Four-Wire Inverter Control Technique for a Single Distributed Generation Unit in Island Mode", IEEE Transactions on Power Electronics, Vol. 23, Issue 1, Jan. 2008, pp. 322 – 331
- [7] Jin-Woo Jung and Ali Keyhani, "Control of a Fuel Cell Based Z-Source Converter", IEEE Transactions on Energy Conversion, Volume 22, No. 2, June 2007, pp. 467-476
- [8] Michael D. Mulligan, Bill Broach, and Thomas H. Lee, "A Constant-Frequency Method for Improving Light-Load Efficiency in Synchronous Buck Converters", Power Electronics Letters, IEEE Volume 3, Issue 1, March 2005 Page(s): 24 - 29
- [9] R.D. Middlebrook and S. Cuk, "A General Unified Approach To Modelling Switching-Converter Power Stages", IEEE Power Electronics Specialists Conference, 1976 Record, pp 18-34.
- [10] Mikkel C. W. Høyerby, Michael A.E. Anderssen, "Envelope Tracking Power Supply with fully controlled 4th order Output Filter", Applied Power Electronics Conference and Exposition, 2006. Twenty-First Annual IEEE, 19-23 March 2006 Page(s): 8 pp. -
- [11] Chin Chang, "Robust Control of DC-DC Converters: The Buck Converter", Power Electronics Specialists Conference, 1995. 26th Annual IEEE Volume 2, Issue , 18-22 Jun 1995 Page(s):1094 - 1097 vol.2
- [12] Mika Sippola and Raimo Sepponen, "DC/DC Converter technology for distributed telecom and microprocessor power systems – a literature review", Helsinki University of Technology Applied Electronics Laboratory, Series E: Electronic Publications E 3, 2002
- [13] Chang, C., "Mixed Voltage/Current Mode Control of PWM Synchronous Buck Converter", Power Electronics and Motion Control Conference, 2004. IPEMC 2004. The 4th International, Publication Date: 14-16 Aug. 2004, Volume: 3, On page(s): 1136- 1139 Vol.3.
- [14] Mohan, Undeland, Robbins Power Electronics – Converters, Applications, and Design 3rd Edition John Wiley & Sons Ltd, 2003
- [15] Rashid, Muhammad H. Power Electronics - Circuits, Devices, and Applications 3rd Edition Pearson Education, 2004
- [16] Walker, Geoff R. "Evaluating MPPT converter topologies using a MATLAB PV model" Australasian Universities Power Engineering Conference, AUPEC '00, Brisbane, 2000
- [17] TT Chow, Zhang GQ, Lin Z, Song CL.: Global optimization of absorption chiller system by genetic algorithm and neural network. Energy Buildings 2002;34:103–9.
- [18] SA Kalogirou "Applications of artificial neural networks in energy systems: a review," Energy Convers Manage 1999; 40:1073–87.
- [19] SA. Kalogirou "Applications of artificial neural networks for energy systems," Appl Energy 2000; 67:17–35.
- [20] SA. Kalogirou "Long-term performance prediction of forced circulation solar domestic water heating Systems using artificial neural networks," Appl Energy 2000; 66:63–74.
- [21] Arzu Sencan, Kemal A.Yakut, Soteris A.Kalogirou " Thermodynamic analysis of absorption systems using artificial neural network," Renewable Energy, Volume 31, issue 1, Jan. 2006, pages 29 – 43.
- [22] A. El Shahat, and H. El Shewy, "PM Synchronous Motor Control Strategies with Their Neural Network Regression Functions", Journal of Electrical Systems, Vol. 5, Issue 4, Dec. 2009.
- [23] Adel El Shahat and Hamed El Shewy, "High Fundamental Frequency PM Synchronous Motor Design Neural Regression Function", Journal of Electrical Engineering, Vol. 10 / 2010 – Edition 1, Article 10.1.14.
- [24] Adel El Shahat, and Hamed El Shewy, "High Speed Synchronous Motor Basic Sizing Neural Function for Renewable Energy Applications", MDGEN05, The International Conference on Millennium Development Goals (MDG): Role of ICT and other technologies December 27 – 29, 2009 in Chennai, India.
- [25] Adel El Shahat, and Hamed El Shewy, "High Speed PM Synchronous Motor Basic Sizing Neural Regression Function for Renewable Energy Applications", Paper ID: X304, Accepted in 2nd International Conference on Computer and Electrical Engineering (ICCEE 2009); Dubai, UAE, December 28 - 30, 2009.
- [26] A. El Shahat, "Generating Basic Sizing Design Regression Neural Function for HSPMSM in Aircraft" EP-127, 13th International Conference on Aerospace Science & Aviation Technology, May 26 – 28, 2009, ASAT 2009 – Military Technical College, Cairo, Egypt.
- [27] Adel El Shahat, and Hamed El Shewy, "High Speed PM Synchronous Motor Basic Sizing Neural Regression Function for Renewable Energy Applications", Paper ID: X304, Accepted in 2nd International Conference on Computer and Electrical Engineering (ICCEE 2009); Dubai, UAE, December 28 - 30, 2009.
- [28] El Shahat, A and El Shewy, H, "Neural Unit for PM Synchronous Machine Performance Improvement used for Renewable Energy", Ref: 93, The Third Ain Shams University International Conference on Environmental Engineering (Ascee- 3), April 14-16 2009, Cairo, Egypt.
- [29] A. El Shahat, H. El Shewy, "Neural Unit for PM Synchronous Machine Performance Improvement used for Renewable Energy", Paper Ref.: 910, Global Conference on Renewable and Energy Efficiency for Desert Regions (GCREEDER2009), Amman, Jordan.
- [30] S. Nafey, A. El Shahat and M. A. Sharaf, "A Neural Model for Flat Plate Collector", EGY- 38, 6th International Conference on Role of Engineering towards a Better Environment, RETBE'06 Conference in Alexandria, 16 - 18 December 2006.

- [31] Adel T. Y. Tawfik, and Adel El Shahat, "A Neuro Modeling for New Biological Technique of Water Pollution Control", EGY-37, 6th International Conference on Role of Engineering towards a Better Environment, RETBE'06 Conference in Alexandria, 16 – 18 December 2006.
- [32] Adel T. Y. Tawfik and Adel El Shahat, "A Neural Model for New Biological Technique of Water Pollution Control: Experimental Project", The 6th Syrian – Egyptian Conference of Chemical & Petroleum Engineering, 8 - 10 November, 2005, Syria.
- [33] A.Y. Tawfik and A. El Shahat, "Speed Sensorless Neural Controller for Induction Motor Efficiency Optimization", 1st International Conference on Advanced Control Circuits and Systems (ACCS'05), ACCS Catalog No: 080610 M 05, ISBN: 0 – 146 – 6310 – 7933 – 2, March 6 – 10, 2005, Cairo, Egypt.
- [34] H. El Shewy, A.Y. Tawfik and A. El Shahat, "Neural Model of 3 phase Induction Motor", 1st International Conference on Advanced Control Circuits and Systems (ACCS'05), ACCS Catalog No: 080610 M 05, ISBN: 0 – 145 – 6310 – 7933 – 2, March 6 – 10, 2005, Cairo, Egypt.
- [35] Schott ASE-300-DGF PV panel data sheet. Source (Affordable Solar website);http://www.affordable-solar.com/admin/product_doc/Doc_pd-00-009-c_ase_300_20080328114646.pdf
- [36] Ali Keyhani, Mohammad N. Marwali, and Min Dai, "Integration of Green and Renewable Energy in Electric Power Systems," Wiley, January 2010
- [37] Masters, Gilbert M. Renewable and Efficient Electric Power Systems John Wiley & Sons Ltd, 2004
- [38] Messenger, Roger & Jerry Ventre Photovoltaic Systems Engineering 2nd Edition CRC Press, 2003
- [39] Castañer, Luis & Santiago Silvestre Modelling Photovoltaic Systems, Using PSpice John Wiley & Sons Ltd, 2002
- [40] Green, Martin A. Solar Cells; Operating Principles, Technology, and System Applications Prentice Hall Inc., 1982
- [41] Walker, Geoff R. "Evaluating MPPT converter topologies using a MATLAB PV model" Australasian Universities Power Engineering Conference, AUPEC '00, Brisbane, 2000
- [42] Adel El Shahat, "PV Cell Module Modeling & ANN Simulation for Smart Grid Applications", Journal of Theoretical and Applied Information Technology, Vol. 16, No.1, June 2010, pp. 9 – 20.